



Automatic Transfer Switching System Base Arduino Nano for Solar Photovoltaic on Railroad Crossing

*Akhwan Akhwan^[1] Sunardi Sunardi^[2], Edi Nyoto Setyo Marsusidi^[3], Dedik Tri Istantara^[4], Erna Utami^[5]

^[1] Indonesian Railway Polytechnic, Madiun, Indonesia

^[2] Politeknik Energi dan Mineral Akamigas, Cepu, Indonesia

*¹akhwan@ppi.ac.id, ²sunardi@ppi.ac.id, ³edi@ppi.ac.id, ⁴dedik@ppi.ac.id, ⁵erna.alern@gmail.com

Abstract. The adequacy of energy supply for transportation purposes with the concept of green energy from renewable sources to replace electricity supply from power utilities still needs to be improved. One of the problems is the energy transfer and management system, because each region has a different energy reserve capacity. To make the system more reliable, an Arduino-based ATS manages the transfer of energy from the source power supply to the battery in the JPL (Direct Railroad Crossing) railway infrastructure to sufficient the electricity demand. When electricity cannot stop supplying at JPL and power outages increase, electricity is supplied from renewable energy sources Solar PV is a potential energy that can be utilized. The suggested solution is to manage many renewable energy sources and adjust the power range according to the needs when the solar heat on minimal until maximum condition in the area where the system can be applied. The researcher used electricity from several Solar PV and utility power supplies to analyze and test the compatibility of the system.

Keywords: ATS, Solar Photovoltaic, Arduino.

1 Introduction

Railroad crossing requires railroad safety infrastructure, as in Bangladesh upgrading the signaling system by using microcontroller technology [1][2]. Railway infrastructure on the direct crossing path (JPL) in the PPI (Indonesian railway polytechnics) Madiun Laboratorium unit has an electrical system, hand generator, and mechanical handle lever. Utilizing Solar Photovoltaic (PV) in converting solar heat into electrical energy [3] to supply the needs of JPL operations. JPL's main power supply electrical energy from Solar PV depends on the availability of sunlight. In the rainy season the power supply requires backup, and transferring the main power supply to backup requires a transfer switch system. Automatic Transfer Switch (ATS) quickly transfers the power supply when the main power source or the supply to the load is interrupted. Microcontroller-based ATS as a control that works based on voltage readings. Using Arduino Nano can simplify the design and minimize the use of components [4].

Indonesia experiences two distinct seasons: dry and rainy. During the dry season, Solar PV systems receive ample sunlight, while the rainy season can negatively affect the ATS system due to reduced irradiation [5]. To optimize solar energy production, it's vital to calculate how many hours of sunlight are available each day using the model in the Solar PV application. To forecast Solar PV power, weather data from the Meteorology, Climatology, and Geophysics Agency's public weather website is used, including temperature, humidity, and wind speed, which are generally consistent across adjacent cities. However, solar radiation can differ due to cloud cover. Nganjuk and Madiun have similar weather patterns, making the data collected from these areas significant in predicting solar PV power demand. The analysis used data from 2012 to 2022, covering an 11-year solar period, and rainfall in the Nganjuk and Madiun regions is illustrated in Figure 1.

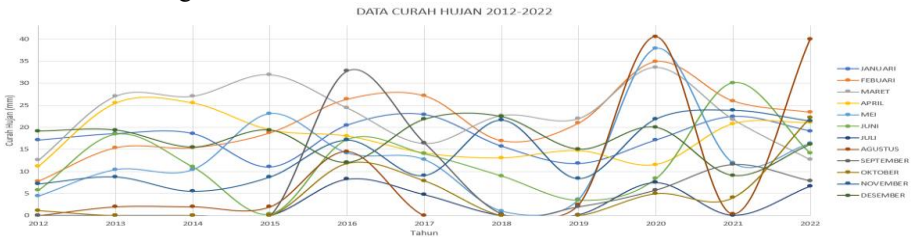


Figure 1. The Data Nganjuk and Madiun rainfall in 2012-2022

It's not uncommon for there to be some months without rainfall, when the conditions are cloudy. Rainfall is classified as light when it ranges from 0.5-20 mm, frequent heavy when it's between 20-50 mm, and very heavy to extreme when it's above 100 mm. The average rainfall in Nganjuk and Madiun is approximately 13.36 mm/month, which suggests that Madiun typically experiences light rain. It's worth noting that rainfall can impact solar irradiation, as shown in Figure 2.

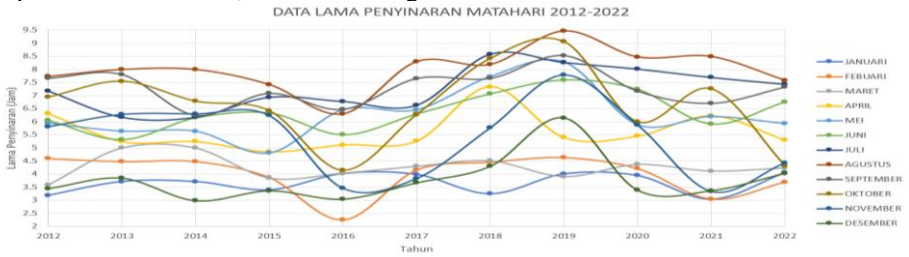


Figure 2 displays the solar irradiation data

There is a correlation between the amount of rainfall and solar irradiation, where an increase in one is often accompanied by a decrease in the other. Solar irradiation duration is measured from sunrise to sunset, and in August, it reaches a peak of approximately 8 hours and 50 minutes per day, compared to only 3 hours and 40 minutes per day in January. The duration of sunshine also impacts temperature conditions, as evidenced by the temperature graph. The graph shows that higher temperatures are observed during periods of greater sunshine, such as in August, while lower temperatures are observed during periods of less sunshine, like in January. Rainfall also affects

temperature fluctuations and has an inverse relationship with sunshine duration. Figure 3 of the temperature graph displays the temperature fluctuations in the Madiun area between 2012 and 2022.

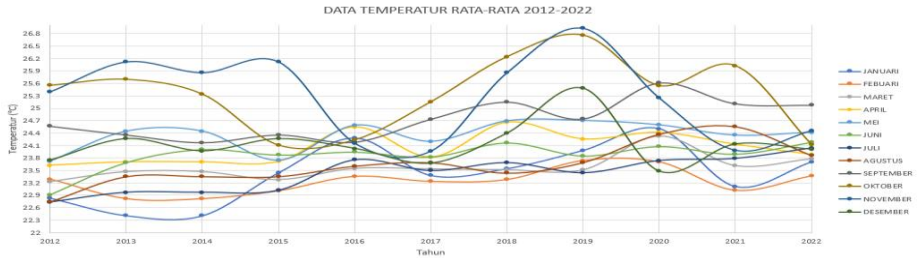


Figure 3. Average temperature of Nganjuk and Madiun in 2012-2022

During the month with the longest duration of sunshine, the highest temperature was recorded in November 2019, reaching almost 27° . However, it's important to note that the length of sunshine does not always correspond to high temperatures. Other factors such as humidity, clouds, and geographical location can influence temperature. In November 2019, despite having shorter sunshine duration than summer months, clear weather conditions, lack of clouds, and geographical features may have contributed to the higher temperatures recorded. Temperature graphs can help understand the complex relationship between sunshine duration and temperature, as well as the various factors that affect temperature changes from month to month. This information is important for optimizing solar PV applications.

JPL, which uses solar PV as its primary power source, faces voltage constraints due to unpredictable weather. To address this, a backup power supply is used for automatic switching of electricity flow between sources[6]. The ATS design uses Arduino to regulate power distribution based on sensor readings when a disturbance is detected[1][7]. ATS power fluctuations are considered to prevent relay flashing and load disturbances[6]. The ATS system based on Arduino Mega 2560 and Triacs is designed to connect loads to generator sets and utility power restoration.[8] Simulation and testing of the ATS system for power supply when utility power source is not detected, startup of backup power supply after a time delay, and detecting utility voltage recovery allows for the load to be switched back to the utility source[4].

2 Automatic Transfer Switch

The Automatic Transfer Switch (ATS) system utilizes voltage sensor readings [2] to switch between the backup power supply and the main power supply when there is a power outage. The Arduino is used to switch on the voltage source from the main power supply, Solar PV, and utility power backup supply for battery charging. The ATS system consists of several components such as a microcontroller, relay module, sensor module, terminal block, solar PV, external charger, battery, and inverter [1][4]. The voltage divider sensor resistor value is calculated to determine the voltage measured, and the resistor value of the calculation that produces input to the Arduino is 5 Volts. The voltage divider formula is used to calculate the sensor value.

$$V_{out} = V_{in} \times \frac{R2}{R1+R2} \dots\dots\dots (1)$$

Verification of calibration or setting the accuracy of measuring instruments by comparing a standard function and its specifications that have been set. Calibration calculation [9] can be achieved by the formula:

$$V_{read} = \frac{(V_{out} \times V_{max\ read})}{Resolusi\ ADC} \dots\dots\dots (2)$$

Where the voltage read (Vread), the output of the voltage divider circuit (Vout), the maximum voltage read by Arduino is 5 Volts DC (Vmax) and the ADC resolution is determined to be 10 Bit (1023). Sensor reading error is calculated to determine accuracy. The error value is minimized by calibration, and becomes a reference to the validity of the measurement with the actual value. The calculation of the error can be known by the following formula:

$$Error = nilai\ terbaca - nilai\ multimeter \dots\dots\dots (3)$$

$$\% \ error = \frac{(nilai\ terbaca - nilai\ multimeter)}{nilai\ terbaca} \times 100\ \% \dots\dots\dots (4)$$

Accurately determining the state of charge (SOC) for a battery requires measuring both its voltage and internal resistance. However, some batteries have voltage levels that can exceed the maximum voltage that an Arduino can read at 5V, reaching up to 24 Volts DC. To address this issue, a voltage divider circuit is employed to reduce the battery voltage to 5 Volts before it enters the microcontroller. This ensures that the microcontroller can precisely read the battery voltage and provide accurate SOC measurements. [8]

The ATS measures the voltage from the Solar PV, battery, and utility power sources. The Arduino receives a sensor output with a current value of 1 Ampere [10]. The relay connects the Solar PV and utility power to the battery. The relay drive circuit is enabled by a signal from the Arduino, which controls the operation. The relay then delivers current to the battery. Solar PV power is maintained to supply the solar charge controller (SCC), and the voltage is kept within permissible limits as per the battery requirement. There are various types of Solar PV, including monocrystalline, shingled monocrystalline, and amorphous, which are known for their efficiency and performance ratio [11][12][13][14]. For this project, Solar PV is used because monocrystalline PV is the most efficient and outperforms the others in terms of several aspects considered.

During the night, the system is powered by the energy stored in the batteries. For certain JPL loads that require an AC source, an inverter is utilized to convert DC to AC. Prior to implementing the ATS, it is important to conduct a simulation to ensure that the device operates as expected. Voltage sensor readings during laboratory simulations may differ from those obtained during JPL tests, and this discrepancy can impact the feasibility of the ATS system during operation.

3 Design Automatic Transfer Switch

Displayed in Figure 4 is the layout of the Arduino ATS, which streamlines the transition of power from the Solar PV and power utility sources to the battery through the use of the Relay block and Sensor block [2]. The control of this process is handled by the Arduino. The Relay block consists of DC contactors, a DC voltage supply block,

and connections for both source and load currents. Meanwhile, the Sensor block is equipped with circuits for measuring the voltage and current of the Solar PV and power utility electrical components utilized in the ATS mechanism.

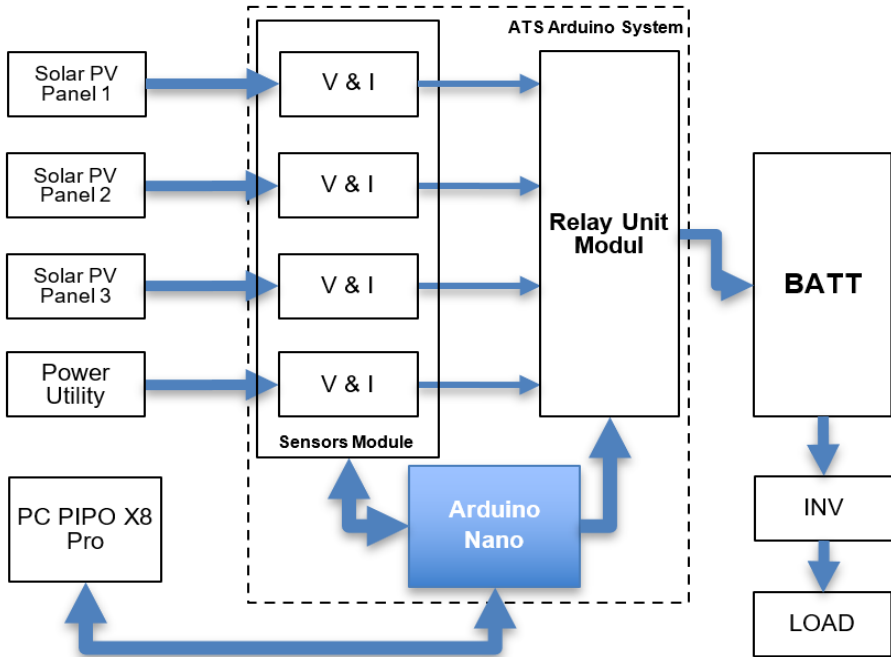


Figure 4. Automatic Transfer Switch Flow Block Diagram

The ATS consists of an Arduino Nano V3 Atmega328P microcontroller that is compact, small, and consumes low power. It has a processor speed of 16 MHz, 32KB flash memory, 2KB SRAM, and 1KB EEPROM. There are 22 digital I/O pins and 6 analog pins available for voltage sensors, current, and contact relay actuators. To enable data communication and monitoring, a serial USB connection is established with the PIPO X8 Pro PC. An external power supply is connected to the Vin pin with an input voltage regulator between 7 to 12 volts. The Integrated Development Environment (IDE) was programmed using Arduino software to write, compile, and upload code to the board. To measure the current source, ACS712-DS 20A [15] was used, which works with the magnetic field generated by the current flowing through the conductor inside. The Hall IC captures the signal and provides a voltage output in analog form. The sensor has an ADC signal that can be read by Arduino. The system interface is monitored by the Windows operating system running on the PIPO X8 Pro PC. The USB ports are used for data communication and monitoring systems to download measurement data in storage media. The ATS schematic is created using Proteus 8 Professional software with configuration settings required for real-time monitoring. The schematic diagram is shown in Figure 5.

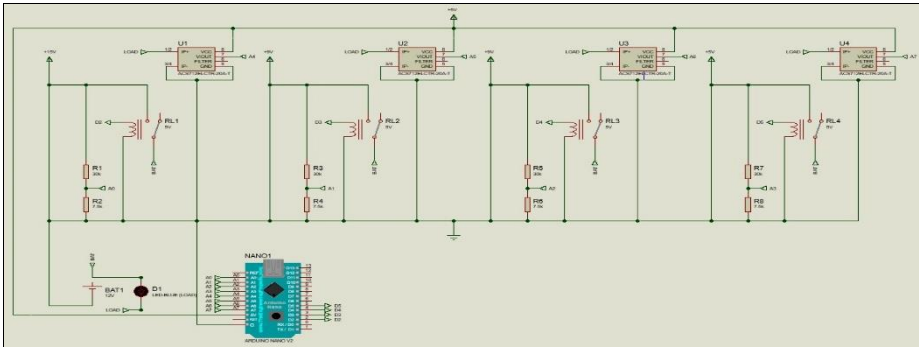


Figure 5. Schematic diagram of Arduino ATS

The driver circuit, documented as ULN2003A, is responsible for controlling the relays RL1, RL2, RL3, and RL4, which can either connect or disconnect the power source line. By closing a specific relay loop, the power supply can be directed towards the load. To enable easy communication with the user and external monitoring, the ATS software has been developed using the Arduino IDE software. The programming includes hardware initialization, switch functions, voltage reading programming, and serial monitor programming. Figure 6 provides a detailed flowchart of the ATS.

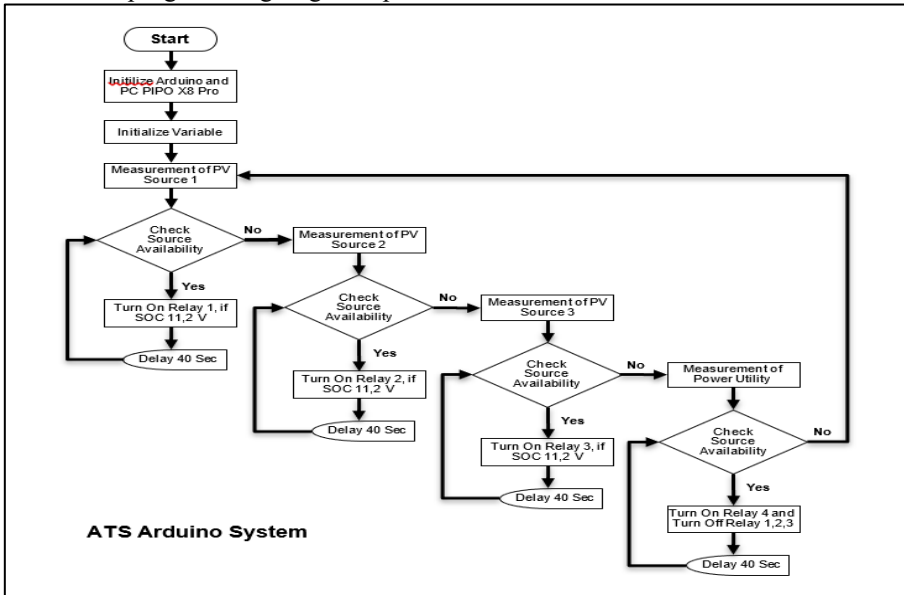


Figure 6. Flowchart of ATS Arduino

In order to ensure optimal battery capacity, the Solar PV voltage is monitored and regulated by an indicator and SCC. The Arduino measures the battery's electrical energy and capacity through a voltage sensor. Once the battery and Solar PV output reach a specified limit during measurement, the relay is instructed to switch the power supply source to the utility by the Arduino. Any voltage problems with the power supplies will prompt the Arduino to send wireless information to the signal and telecommunication

operator. ATS is tested through simulation to determine performance and errors. SOC determines whether the load can receive power from the battery, but only if it is above 35% supplied from Solar PV. If it is below 30%, the power utility supply is used after exhausting Solar PV units 1, 2, 3, and 4. The SOC percent is checked to determine when the battery voltage decreases and the supply mode needs to change. The SOC percent, determined from the power utility voltage, is checked every 40 seconds to ensure a proper source supply. In the absence of power utility supply, the load relies on the battery. The Arduino checks the battery condition and supplies the load accordingly, based on the sensed SOC and acceptable limits.

4 Prototype of Arduino

The prototype of the Arduino ATS is housed in a box made of Acrylonitrile Butadiene Styrene (ABS). Inside the box, you'll find Arduino components, relay modules, voltage and current sensor blocks, and power supplies. The PC unit is located outside the box, on the door lid. Refer to Figure 7 for a visual of the prototype.



Figure 7. Prototype of ATS Arduino

The ATS prototype was tested to convert the available solar energy in place of utility power. The uncertainty of current and voltage of multi-junction Solar PV needs to be known for calibration to determine the connecting at the same load, because the efficiency of energy conversion depends on temperature based on monocrystalline silicon in the range with extreme limits from -40° to 185°F at the earth's surface. The risk of system failure in a realistic concept of ATS design using this software, we arrange multi junction and multi connecting to know the characteristics of current and voltage in a particular area and purpose. The research was conducted to provide recommendations for the right components for the Madiun and Nganjuk areas for the provision of new renewable electricity resources in the JPL railway infrastructure.

5 Simulation Result

In order to accurately measure the voltage of a Solar PV, two resistors must be connected in series to produce an input voltage of 5 Volts for an Arduino. Specifically, R1 should be 68 k Ω and R2 should be 10 k Ω , resulting in an output of 5.1 Volts for a 40 Volts Solar PV. Alternatively, using R1 of 47 k Ω and R2 of 9.1 k Ω will produce an output of 4.9 Volts for a 30 Volts Solar PV. To ensure precise readings, voltage sensors are necessary for all energy sources utilized in the system, with voltage divider resistor values of 30 k Ω and 7.5 k Ω for a battery charging voltage limit of 11.2 volts. The accuracy of the input voltage reading is calibrated using a formula integrated into the Arduino IDE program. When properly calibrated and configured, the Arduino can accurately measure the output voltage of the Solar PV, enabling effective monitoring of its performance at JPL. All calibration data for voltage sensor readings is recorded in Table 1.

Table 1. Arduino Nano analog voltage bit readings

Analog Voltage	Arduino Nano ADC Resolution	Voltage Read
0 Volt	0	0 Volt
1 Volt	200,60	8 Volt
2 Volt	401,20	16 Volt
3 Volt	601,80	24,1 Volt
4 Volt	802,40	32,1 Volt
5,1 Volt	1023,06	40,9 Volt

Table 1, the voltage measured by the analog pin on the Arduino is recorded. This measurement is taken to account for the decrease in output voltage of the Solar PV, ensuring that the voltage entering the analog pin stays within the Arduino input range. Once calibration is complete, the analog voltage is processed through ADC and represented in bit form. This process allows for the conversion of the ADC value back to the original voltage, based on the actual scale. The ADC value provides information on the original measured voltage and can be further processed by the Arduino to accurately measure the Solar PV voltage. It's worth noting that the voltage with ADC value is linear, meaning that the value doesn't change based on calibration results.

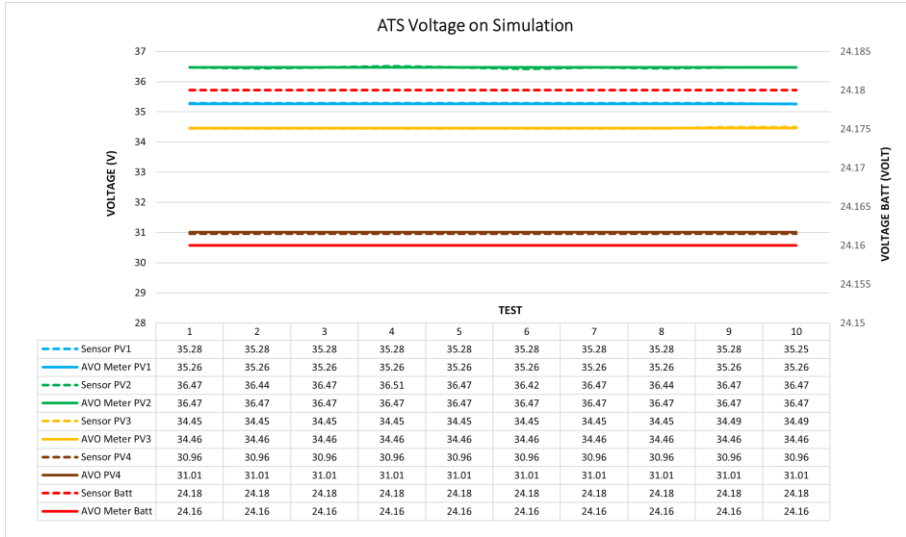


Figure 8. Simulation of ATS voltage reading

Figure 8 displays the voltage difference in the Solar PV1 simulation. The voltage sensor reading and the multimeter indicate a range of 35.28 to 35.26 volts. The simulated voltage of Solar PV2 ranges from 36.44 to 36.51 volts with a value of 36.47 volts. For Solar PV3, the value range is 34.45 to 34.46 volts, and for Solar PV4, the voltage range is 30.96 to 31.01 volts. The voltage reading range of the battery from the sensor and AVO meter is 24.18 to 24.16 volts. The voltage sensor readings on the serial monitor are obtained from the voltage divider resistor values. These values allow for outputs up to 30 volts DC based on the maximum capacity of the battery installed at JPL, with a maximum V_{out} result of 5 volts DC. Table 2 presents the calibration results and voltage sensor readings, where a resistor value of R1 47 k Ω with R2 9.1 k Ω was used.

Table 2. Arduino Nano Analog Voltage Bit Reading

Analog Voltage	Arduino Nano ADC Resolution	Voltage Read
0 Volt	0	0 Volt
1 Volt	208,7	6,1 Volt
2 Volt	417,5	12,2 Volt
3 Volt	636,3	18,6 Volt
4 Volt	835	24,4 Volt
4,9 Volt	1023	30 Volt

This system displays the voltage that enters the Arduino analog pin and the resulting ADC bit from calibration. This allows for an accurate reading of the original voltage. The ADC value remains constant, unaffected by calibration. The transfer of power supply from Solar PV to battery charging is determined by the voltage sensor reading at the output of Solar PV and battery. This process is influenced by weather and sunlight intensity. If the Solar PV output is optimal, the battery will charge from it. However, if the Solar PV output falls below a predetermined tolerance value, and the battery is at a low capacity, the electrical energy supply will switch to the power utility through a relay. The Arduino controls the transfer of power supply and sends voltage to an

external relay block. Two relays work in the normally open (NO) position for this power transfer.

Table 3. Power supply displacement testing

Test	Voltage (V DC)		Starting Condition	Switching	Final Result
	Solar cell	Battery			
1	27,87	26,53	Solar Panel	No	Solar Panel
2	32,54	18,24	External Charger	Yes	Solar Panel
3	28,89	18,38	Solar Panel	Yes	External Charger
4	27,41	24,14	Solar Panel	No	Solar Panel
5	27,56	19,29	Solar Panel	No	Solar Panel
6	29,80	23,09	Solar Panel	No	Solar Panel
7	33,04	22,71	Solar Panel	No	Solar Panel
8	28,89	19,80	External Charger	No	External Charger
9	30,25	19,53	External Charger	Yes	Solar Panel
10	29,02	19,58	Solar Panel	Yes	External Charger

The power supply switching test shows the initial condition before switching to the final Result based on the voltage test sensor reading. If the battery capacity is less than 20 Volts and the solar PV voltage output is less than 30 Volts, the power supply comes from the power utility. If the output voltage of the solar PV is more than 30 Volts, the power supply comes from the solar PV.

6 The Testing of Results at JPL

Once the voltage readings on the ATS voltage sensor have been simulated, the next step is to test the JPL equipment, which includes Solar PV and batteries. The voltage readings under load conditions at JPL PPI Madiun are shown in Figure 9 below.

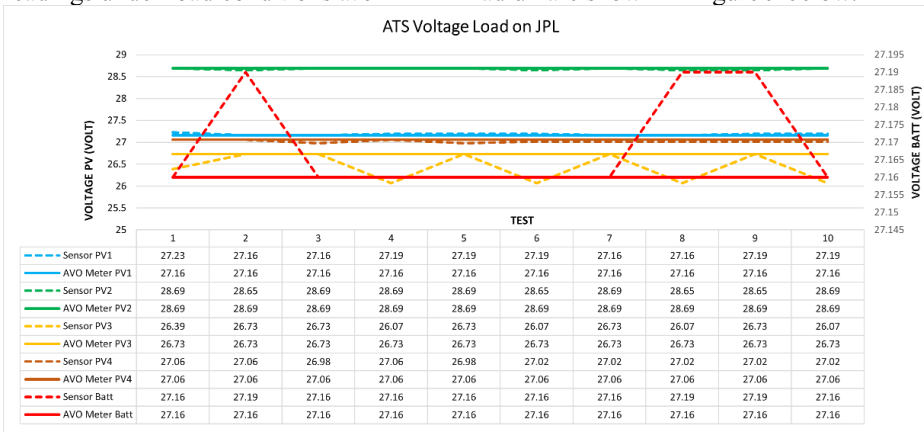


Figure 9. ATS testing at JPL PPI Madiun

Figure 9 displays the voltage difference in the Solar PV1 load test at JPL PPI Madiun. The voltage sensor reading with a multimeter ranged from 27.16 to 27.23 volts, while the reading from the voltage sensor alone was 27.16 volts. For the Solar PV2 load testing, the voltage range was between 28.65 and 28.69 volts, with a reading of 28.69 volts. The Solar PV3 range of values was between 26.07 and 26.98 volts, with a reading of 26.73 volts. Solar PV4 had a voltage range of 26.98 to 27.06 volts, with a reading of

27.06 volts. The battery's voltage readings from the sensor and AVO meter ranged from 27.16 to 27.19 volts, with a reading of 27.16 volts. The Solar PV load testing passed the calibration process on the serial monitor for voltage readings from sensors and multimeters on the ATS system voltage divider circuit JPL PPI Madiun [16]. During the testing phase on JPL equipment, the battery also underwent the calibration process.

7 Comparison of Voltage Sensor Errors

To ensure the feasibility of any changes when installed on JPL equipment, errors were compared to determine the deviation between simulation and testing. Figure 10 below shows the error between voltage readings during simulation and testing. The error difference between solar PV1 during laboratory simulation and direct testing at JPL PPI Madiun is relatively small, reaching a value of 0.20%. Similarly, the error comparison of solar PV2 reached a value of 0.11%, and the battery error comparison reached a value of 0.08%. However, the error comparison of solar PV3 reached a value of 2.4%, and the error comparison of solar PV4 reached 0.16%. Judging from the total error comparison graph, the error difference reached 2.4%, indicating that the errors during simulation and testing are not significantly different. Therefore, the ATS condition has not changed from the initial condition during the simulation.

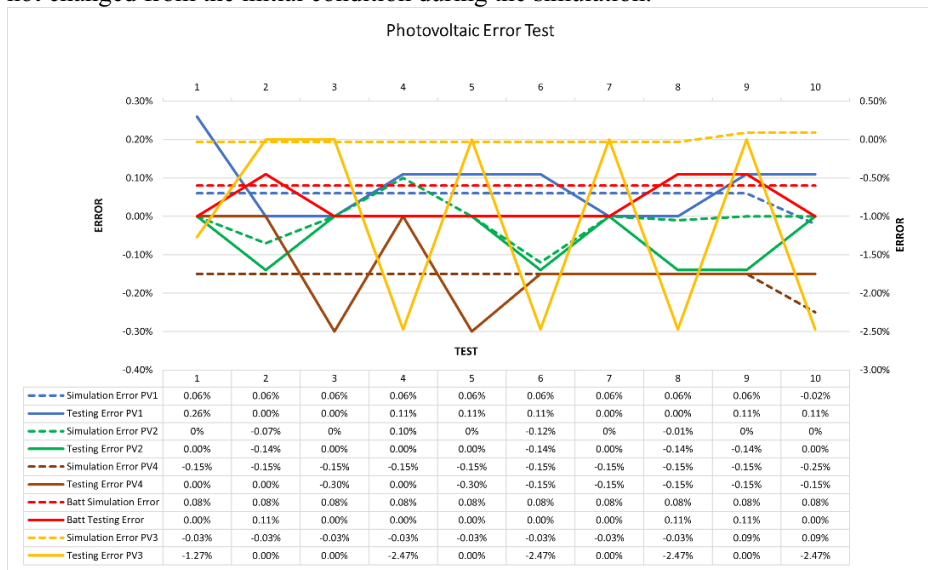


Figure 10. Comparison of Voltage Sensor Errors

8 Conclusion

The Automatic Transfer Switch (ATS) at JPL PPI Madiun is designed to switch the voltage source between the Solar PV power supply and the utility power supply for battery charging. Two relay circuits drain the voltage from the power supply source to

charge the battery. The Arduino Nano control device reads the voltage sensor, which is installed at the output of the solar PV source, power utility, and battery as a reference for switching power supplies. The resistor values for the solar PV voltage sensor are 68 k Ω and 10 k Ω , while for the battery voltage sensor, they are 47 k Ω and 9.1 k Ω . The voltage divider circuit outputs 5 volts to the ADC pin of the Arduino Nano, which displays the actual voltage value on the serial monitor. If the battery capacity drops below 20 volts, the Arduino Nano provides information about the battery status. In simulation and testing at JPL PPI Madiun, the ATS tool's error value difference is 2.4%, indicating that it has not changed from the initial planning.

References

- [1] K. R. Ahmed, M. A. Hossain, A. Akter and L. Akthar, "A Secure Automated Level Crossing and Train Detection System for Bangladesh Railway," 2022 International Conference on Advancement in Electrical and Electronic Engineering (ICAEEE), Gazipur, Bangladesh, 2022, pp. 1-4, doi: 10.1109/ICAEEE54957.2022.9836361.
- [2] P. Bhowmik, S. Islam, J. K. Sifat, M. d. S. Mahmud and F. Faisal, "Design and Development of IoT based Automated Railway Level Crossing," 2022 6th International Conference on Trends in Electronics and Informatics (ICOEI), Tirunelveli, India, 2022, pp. 01-06, doi: 10.1109/ICOEI53556.2022.9776956.
- [3] Sunardi, S. S., Su'udy, A. H., Cundoko, A., & Istiantara, D. T. (2021). Optimalisasi Pemanfaatan SHM (Solar Home System) Sebagai Pembangkit Energi Listrik Ramah Lingkungan. *Eksergi*, 17(2), 76. <https://doi.org/10.32497/eksergi.v17i2.2165>
- [4] Principles, A. T. W. (2018). Arduino-based Automatic Transfer Switch for Domestic Emergency Power Generator-Set A must for an area with frequent electricity service interruption. 2018 2nd IEEE Advanced Information Management, Communicates, Electronic and Automation Control Conference (IMCEC), Imceec, 742–746.
- [5] M. S. Hossain and H. Mahmood, "Short-term photovoltaic power forecasting using an LSTM neural network and synthetic weather forecast," *IEEE Access*, vol. 8, pp. 172524–172533, 2020, doi: 10.1109/ACCESS.2020.3024901..
- [6] Azeem, M. Q., Habib-Ur-Rehman, Ahmed, S., & Khattak, A. (2017). Design and analysis of switching in automatic transfer switch for load transfer. *ICOSST 2016 - 2016 International Conference on Open Source Systems and Technologies, Proceedings*, 129–134. <https://doi.org/10.1109/ICOSST.2016.7838589>.
- [7] Choi, M. S., Lim, I. H., Trirohadi, H., & Lee, S. J. (2011). An optimal location of automatic switches for restorable configuration in distribution automation systems. *APAP 2011 - Proceedings: 2011 International Conference on Advanced Power System Automation and Protection*, 3, 1938–1942. <https://doi.org/10.1109/APAP.2011.6180761>
- [8] Alembong, M., Essiet, I.O., & Sun, Y. (2021). Swift Automatic Transfer Switch based on Arduino Mega 2560, Triacs Bluetooth and GSM. 2021 International

- Conference on Sustainable Energy and Future Electric Transportation (SEFET), 1-6.
- [9] F. Guo, Z. Jiang, Y. Wang, C. Chen and Y. Qian, "Dense Traffic Detection at Highway-Railroad Grade Crossings," in *IEEE Transactions on Intelligent Transportation Systems*, vol. 23, no. 9, pp. 15498-15511, Sept. 2022, doi: 10.1109/TITS.2022.3140948.
- [10] Prakash, A. (1997). A logic of corporate environmentalism: "Beyond-compliance" environmental policymaking in Baxter International Inc. and Eli Lilly and Company. ProQuest Dissertations and Theses, VI (01), 329.
- [11] A. Vigneswaran, M. S. Majid, H. A. Rahman, M. Y. Hassan and M. K. Hamzah, "Cost comparison between Amorphous Silicon and cadmium telluride for stand-alone photovoltaic system in Malaysia," 2008 IEEE 2nd International Power and Energy Conference, Johor Bahru, Malaysia, 2008, pp. 468-472, doi: 10.1109/PECON.2008.4762511.
- [12] L. Jiang, S. Cui, P. Sun, Y. Wang and C. Yang, "Comparison of Monocrystalline and Polycrystalline Solar Modules," 2020 IEEE 5th Information Technology and Mechatronics Engineering Conference (ITOEC), Chongqing, China, 2020, pp. 341-344, doi: 10.1109/ITOEC49072.2020.9141722.
- [13] M. Lee, L. Ngan, W. Hayes and A. F. Panchula, "Comparison of the effects of spectrum on cadmium telluride and monocrystalline silicon photovoltaic module performance," 2015 IEEE 42nd Photovoltaic Specialist Conference (PVSC), New Orleans, LA, USA, 2015, pp. 1-4, doi: 10.1109/PVSC.2015.7356174.
- [14] J. H. Romoacca, A. P. Lopez, F. Palomino-Quispe and R. J. Coaquira-Castillo, "Study of the effect of temperature on electrical performance in monocrystalline and polycrystalline photovoltaic systems in Cusco-Peru," 2021 IEEE XXVIII International Conference on Electronics, Electrical Engineering and Computing (INTERCON), Lima, Peru, 2021, pp. 1-4, doi: 10.1109/INTERCON52678.2021.9532808.
- [15] Chang, L. X., Yu, C. H., Luo, Y. F., & Gong, C. S. A. (2013). A fully integrated solar charger controller with input MPPT regulation protection for 10V to 28V solar-powered panel. *Proceedings of the International Symposium on Consumer Electronics, ISCE*, 2, 11–12. <https://doi.org/10.1109/ISCE.2013.6570134>.
- [16] Sunardi, Teguh Arifianto, Willy Artha Wirawan, Wahyu Tamtomo Adi, Ayi Syaeful Bahri; Geoelectric survey for reactivation planning from Madiun-Slahung railway track in Indonesia. *AIP Conference Proceedings* 9 March 2023; 2671 (1): 020004. <https://doi.org/10.1063/5.0116640>

Open Access This chapter is licensed under the terms of the Creative Commons Attribution-NonCommercial 4.0 International License (<http://creativecommons.org/licenses/by-nc/4.0/>), which permits any noncommercial use, sharing, adaptation, distribution and reproduction in any medium or format, as long as you give appropriate credit to the original author(s) and the source, provide a link to the Creative Commons license and indicate if changes were made.

The images or other third party material in this chapter are included in the chapter's Creative Commons license, unless indicated otherwise in a credit line to the material. If material is not included in the chapter's Creative Commons license and your intended use is not permitted by statutory regulation or exceeds the permitted use, you will need to obtain permission directly from the copyright holder.

